JOURNAL OF VIROLOGY, Nov. 2007, p. 12348–12359 Vol. 81, No. 22
0022-538X/07/$08.00+0 doi:10.1128/JVI.01177-07

Morphogenesis of a Highly Replicative EGFPVP22 Recombinant Marek's Disease Virus in Cell Culture[▽]

C. Denesvre,[1]* C. Blondeau,[1] M. Lemesle,[3] Y. Le Vern,[2] D. Vautherot,[1] P. Roingeard,[3] and J. F. Vautherot[1]

Laboratoire de Virologie Moléculaire, INRA, UR1282, Infectiologie Animale et Santé Publique, IASP, Nouzilly 37380, France[1]*; Service Commun de Cytométrie, Centre INRA de Tours, 37380 Nouzilly, France*[2]*; and Université François Rabelais, INSERM ERI 19, Faculté de Médecine & CHRU, 10 boulevard Tonnelé, 37032 Tours, France*[3]

Received 30 May 2007/Accepted 4 September 2007

Marek's disease virus (MDV) is an alphaherpesvirus for which infection is strictly cell associated in permissive cell culture systems. In contrast to most other alphaherpesviruses, no comprehensive ultrastructural study has been published to date describing the different stages of MDV morphogenesis. To circumvent problems linked to nonsynchronized infection and low infectivity titers, we generated a recombinant MDV expressing an enhanced green fluorescent protein fused to VP22, a major tegument protein that is not implicated in virion morphogenesis. Growth of this recombinant virus in cell culture was decreased threefold compared to that of the parental Bac20 virus, but this mutant was still highly replicative. The recombinant virus allowed us to select infected cells by cell-sorting cytometry at late stages of infection for subsequent transmission electron microscopy analysis. Under these conditions, all of the stages of assembly and virion morphogenesis could be observed except extracellular enveloped virions, even at the cell surface. We observed 10-fold fewer naked cytoplasmic capsids than nuclear capsids, and intracellular enveloped virions were very rare. The partial envelopment of capsids in the cytoplasm supports the hypothesis of the acquisition of the final envelope in this cellular compartment. We demonstrate for the first time that, compared to other alphaherpesviruses, MDV seems deficient in three crucial steps of viral morphogenesis, i.e., release from the nucleus, secondary envelopment, and the exocytosis process. The discrepancy between the efficiency with which this MDV mutant spreads in cell culture and the relatively inefficient process of its envelopment and virion release raises the question of the MDV cell-to-cell spreading mechanism.

Marek's disease virus (MDV), referred to as *Gallid herpesvirus 2*, is the etiological agent of Marek's disease in chickens, a multifaceted disease most widely recognized by the induction of a malignant T-cell lymphoma. This major pathogen of chickens is a herpesvirus classified in the *Mardivirus* genus (Marek's disease-like viruses) within the *Alphaherpesvirinae* subfamily. MDV can be efficiently propagated in cell culture but remains strictly cell associated without free viral particles being detectable in the supernatant (2, 38). Moreover, infectious MDV virion particles cannot be purified from infected cell lysates as has been described for varicella-zoster virus (VZV) or turkey herpesvirus. Therefore, homologous vaccines commonly used in poultry flocks are frozen viable MDV-infected cells, which require storage and transport in liquid nitrogen (4). This feature makes MDV a unique virus within the herpesvirus family and among animal viruses in general.

From electron microscopy (EM) studies of cultured cells infected with various herpesviruses, including mutant viruses with deletions of different tegument proteins or glycoproteins genes, three different pathways for the assembly and morphogenesis of herpesviruses have been proposed (reviewed in references 7, 20, 27, 34, and 35). The assembly process begins in the nucleus, where the viral genome is packaged into capsids, resulting in C capsids. Then, nucleocapsids exit from the nucleus to the cytoplasm. In the first scenario, called the double-envelopment model, it is assumed that this process involves a primary envelopment at the inner membrane of the nuclear envelope, followed by a fusion at the outer membrane, releasing the capsids into the cytoplasm. Then, the cytosolic capsids bind several tegument proteins through a process called tegumentation and are reenveloped by budding into cytoplasmic vesicles derived from the trans-Golgi network or the endosomes. The final egress step probably occurs through exocytosis of vesicles. Recently, a second route of egress from the nucleus to the cytoplasm was proposed for bovine herpesvirus 1 and herpes simplex virus type 1 (HSV-1); this route of egress involves dilatation of the nuclear pores, resulting in direct access of capsids to the cytoplasm (31, 50). A third model of egress, called the "lumenal" model was proposed for HSV-1. In this model, egress starts with the same initial event of nucleocapsid budding at the inner leaflet of the nuclear envelope but is followed by virion transport through the endoplasmic reticulum and via the secretory pathway toward the cell surface. In this model, cytosolic naked capsids will never mature into infectious particles (6). Discussions of these three egress pathways are still occurring in the literature (8, 36, 37, 48, 49). None of these scenarios has been validated to date for MDV, which presents some peculiarities in its biological properties compared to the other alphaherpesviruses. Several EM studies in the 1960s and 1970s showed the presence of typical herpesvirus capsids in the nuclei of cultured cells producing MDV (10, 39, 40) or in tissues from MDV-infected chickens (9, 12,

* Corresponding author. Mailing address: Laboratoire Virologie Moléculaire, INRA, UR1282, Infectiologie Animale et Santé Publique, IASP, Nouzilly F-37380, France. Phone: (33) 2 47 42 76 19. Fax: (33) 2 47 42 77 74. E-mail: denesvre@tours.inra.fr.

▽ Published ahead of print on 12 September 2007.

28). MDV enveloped particles were observed in negatively stained preparations from lysed feather follicle epithelium (5). A recent study supports the hypothesis of a primary envelopment process for MDV (46). In this report, the absence of the U_S3-encoded protein kinase resulted in the accumulation of primary enveloped virions in the perinuclear space, which is consistent with recent observations made with pseudorabies virus (PRV) and HSV-1 (23, 43).

The UL49 gene is conserved throughout the subfamily *Alphaherpesvirinae*. The MDV UL49 gene encodes VP22, a major tegument protein consisting of 249 amino acids (aa) with an apparent molecular mass of 30 to 32 kDa. We have previously demonstrated that the VP22 protein is abundantly expressed in MDV-infected chicken embryonic skin cells (CESCs) (15). Moreover, we were able to show that when the MDV UL49 gene is replaced with a kanamycin resistance gene in infectious bacterial chromosome clone Bac20, the resulting recombinant Bac20ΔUL49 is completely unable to spread in cell culture (16). This absolute requirement of UL49 for virus spread was not observed in any of the other alphaherpesviruses studied (PRV, HSV-1, BHV-1), except very recently in VZV (14, 17, 18, 32; X. Che, M. Sommer, L. Zerboni, J. Rajamani, and A. M. Arvin, 32nd International Herpesvirus Workshop, 2007). However, in some replication systems, an HSV UL49-null mutant can be dramatically impaired in its spreading (17). The role of VP22 in virus infection remains unclear. For HSV-1 and VZV, one of its roles could be indirect by the recruitment of other tegument proteins such as ICP0, ICP4 HSV-1/IE62 VZV, and glycoproteins (gB, gD, gE) into infectious virion particles that are involved in the early phase of infection (11, 17, 18). The absence of VP22 has not been associated with a blockade of virion morphogenesis, and VP22 is not considered to be required for virion formation (14, 21, 35).

Direct examination of cells infected with MDV by transmission EM (TEM) has always been cumbersome and unsatisfactory, revealing mostly nuclear capsids. This is probably due to a relatively small percentage of infected cells and to the lack of synchronization of the infection, with cells at all stages of infection, including early stages. Our aim was therefore to perform TEM exclusively on infected cells at late stages of infection. To this end, we engineered a fluorescent MDV mutant in which the late VP22 protein is fused to the C terminus of the enhanced green fluorescent protein (EGFP). Despite a reduction in virus growth, confirming the potential role of MDV VP22 in cell-to-cell spreading, this mutant virus was still highly replicative and allowed sorting of MDV fluorescent cells by cytometry. TEM of these selected cells showed all of the virion forms described in herpesvirus morphogenesis, with the exception of extracellular virions, confirming that this extracellular form is very rare or nonexistent in cell culture for MDV. Moreover, counting of the various intracellular particle types demonstrates that nuclear egress and secondary envelopment in the cytoplasm are inefficient processes in MDV morphogenesis.

MATERIALS AND METHODS

Cells and viruses. CESCs from 12-day-old LD1 or B19ev0 chicken embryos were prepared and cultured as previously described (15). Twenty-four hours after seeding, CESCs were supplemented with 1 mg/ml *N*,*N*′-hexamethylene bisacetamide (Sigma, St. Louis, MO). The parental Bac20 virus was reconstituted from Bac20 DNA by calcium phosphate transfection into CESCs (45).

Antibodies. Two mouse monoclonal antibodies (MAbs) against MDV antigens were used, F19 (immunoglobulin G1) against capsid protein VP5 and L13a against tegument protein VP22 (3, 16). Mouse JL-8 MAb no. 8371-1 and rabbit polyclonal antibody no. 632459, both directed against GFP, were used (BD Biosciences Clontech, Mountain View, CA). A mouse H52 MAb to hepatitis C virus (anti-E2 protein) was used as an irrelevant control antibody (kind gift of J. Dubuisson). The rabbit anti-mouse Alexafluor 594 secondary antibody (Invitrogen), phosphatase-conjugated secondary antibodies (Sigma), and gold-conjugated secondary antibodies (BBInternational, Cardiff, United Kingdom) were used for immunofluorescence, Western blotting, and immuno-EM, respectively.

Primers. The primers used in this study are available upon request.

BACmid and plasmids. pBac20ΔUL49 was described earlier (16). Briefly, in the genome of attenuated MDV strain 584Ap80C cloned as a bacterial artificial chromosome (Bac20), the UL49 gene was replaced with a kanamycin resistance gene through homologous recombination in *Escherichia coli*.

Construction of the EGFPUL49 fusion gene. The MDV UL49 gene was amplified by PCR from plasmid pcDNA3 VP22 (15) with primers MDV37f′ and MDV37r, resulting in a 766-bp fragment which incorporated BglII and HindIII sites at the 5′ and 3′ ends, respectively, of UL49, thereby replacing the ATG of the UL49 gene with a TTG codon. This PCR fragment was cloned into pGEM-Te (Promega, Madison, WI) to generate pGEM-BglIIUL49HdIII. The 762-bp BglII-HindIII fragment of pGEM BglIIUL49HdIII was subcloned into plasmid pEGFP-C1 (BD Biosciences Clontech) by using the BglII and HindIII sites, resulting in the pEGFPUL49 plasmid. In order to introduce a unique StuI site at the 5′ end of the EGFPUL49 gene, the EGFPUL49 fusion gene was amplified by PCR from plasmid pEGFPUL49 by using primers stuIEGFPf and MDV37r; this resulted in a 1,498-bp fragment which was cloned into pGEM-Te, yielding plasmid pGEM-StuEGFPUL49. The EGFPUL49 gene encoded a 493-aa protein with 239 aa corresponding to EGFP, 5 aa corresponding to a spacer, and 249 aa corresponding to VP22. The methionine of VP22 corresponding to the start codon was replaced with a leucine.

Construction of shuttle plasmid pUL48-49 EGFPUL49. Two contiguous regions of the oncogenic MDV RB-1B strain were amplified by PCR from DNA derived from primary lymphoma by using primers 48f and 49r or 49.5f and 50r; this amplification yielded two fragments, (i) a 2,389-bp fragment containing the UL48 and UL49 genes incorporating an EcoRI site at one end and an StuI site at the other end immediately 5′ of the UL49 ATG and (ii) a 1,735-bp fragment containing the UL49.5 and UL50 genes and incorporating an StuI site at one end and an NruI site at the other. Both PCR fragments were inserted into pGEM-Te (Promega) to generate p48-49 Stu and pStu 49.5-50. The 1.7-kbp StuI-NotI fragment of pStu 49.5-50 was inserted into p48-49 Stu in order to produce plasmid pUL48-50 Stu (7.11 kb). This plasmid contains the UL49 gene with an StuI site immediately upstream of the ATG and the UL49 flanking sequences including the UL48, UL49.5, and UL50 genes. The UL49 gene was then replaced with the EGFPUL49 fusion gene. To this end, the 1,145-bp StuI-BssHII fragment of pGEM-StuEGFPUL49 was ligated with the StuI-BssHII fragment of plasmid pUL48-50, resulting in plasmid pUL48-50 EGFPUL49, the shuttle plasmid. The final construct was verified by DNA sequencing (MWG Biotech Sequencing Service, Ebersberg, Germany).

Generation of a recombinant MDV that expresses EGFPVP22. To obtain a mutant MDV that expresses EGFPVP22, 1.5 μg of pUL48-50 EGFPUL49 and 3 μg of Bac20ΔUL49 BACmid DNA were transfected into CESCs grown in 60-mm dishes by the calcium phosphate precipitation method (30). Six days later, one-third of the trypsinized transfected cells were used to infect fresh CESCs grown in a 60-mm dish. The infected cells were then harvested, and the fluorescent virus was amplified on fresh CESCs. The genome of the recombinant Bac20 MDV expressing the EGFPVP22 protein, named Bac20 EGFPVP22, is schematically represented in Fig. 1A. The recombinant virus used in this study never exceeded six passages in cell culture.

Viral DNA analyses. Viral DNA was purified from approximately 0.5×10^7 to 1×10^7 infected CESCs grown in a 100-mm dish as described previously (47) and amplified by PCR with primers car4 and car6 located in UL49 flanking sequences. The PCR product was purified with the Quick-Clean kit (Bioline, London, United Kingdom) and directly sequenced on both strands (MWG Biotech) with primers car4 and car6 (primer information available upon request).

VP22 Western blot analysis. For Western blot assays, 0.5×10^7 to 1×10^7 infected or uninfected control CESCs were trypsinized, pelleted by centrifugation, and lysed in 2× Laemmli sample buffer. The samples were boiled and sonicated. Solubilized proteins were subjected to sodium dodecyl sulfate-polyacrylamide gel electrophoresis and transferred to nitrocellulose membranes. The membranes were then incubated with either the rabbit anti-EGFP antibody or

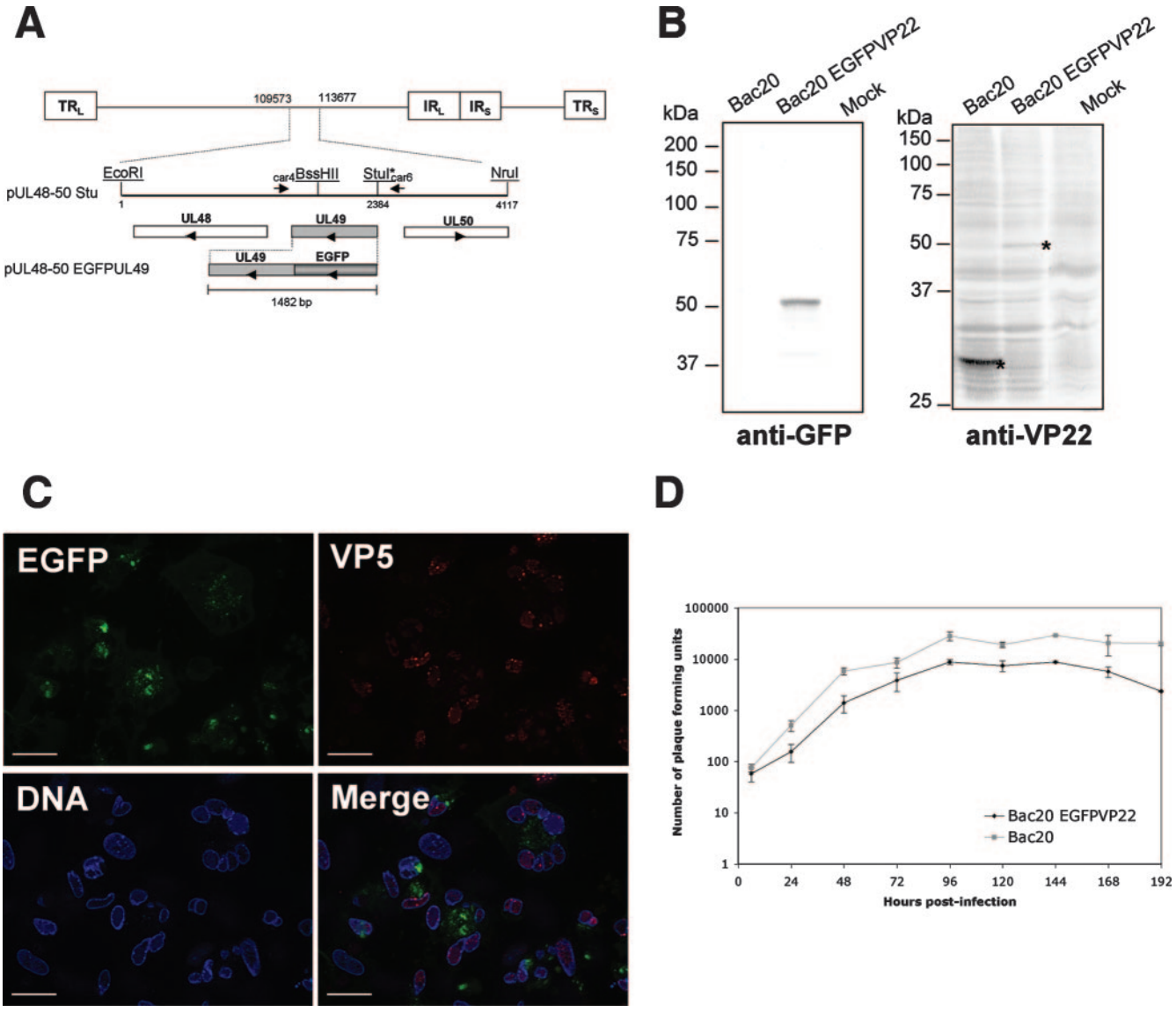

FIG. 1. Generation and characterization of recombinant MDV expressing EGFPVP22. (A) Schematic representation of the MDV genome. The 4,117-bp EcoRI-NruI fragment (positions 109573 to 113677 in the Md5 sequence, accession no. AF243438), containing an StuI restriction site inserted immediately upstream of the UL49 start codon, was cloned into pGEM-Te to yield plasmid pUL48-50 Stu. This plasmid contains UL49 and its flanking sequences derived from the RB1B genome. Arrowheads indicate the direction of gene transcription. The construct pUL48-50 EGFPUL49 containing the EGFP coding region fused to the 5′ end of the MDV UL49 open reading frame in the same plasmid backbone is also shown. (B) Analysis of EGFPVP22 protein expression by Western blotting. CESCs infected with the Bac20 EGFPVP22 or the parental Bac20 virus were trypsinized 5 days postinfection, pelleted by centrifugation, and directly lysed in 2× Laemmli buffer. Sonicated crude cell lysates were separated by sodium dodecyl sulfate-polyacrylamide gel electrophoresis on a 10% polyacrylamide gel and transferred to nitrocellulose. The blots were incubated with the rabbit anti-GFP antibody or the L13a anti-VP22 MAb. Mock corresponds to noninfected cells. The molecular mass marker positions (molecular mass are in kilodaltons) are indicated on the left. The molecular mass of the EGFPVP22 protein was estimated on the gel at 50 kDa. (C) Fluorescence analysis on CESCs infected with the Bac20 EGFPVP22 virus. Cells were infected on coverslips and fixed at 5 days postinfection. EGFPVP22 was visualized via EGFP fluorescence (green), the VP5 major capsid protein was stained with the F19 MAb (red), and the nuclei were stained with Hoechst 33342 dye (blue). Cells were examined under a Zeiss microscope with the ApoTome system. EGFPVP22 was found in both the cytoplasmic and nuclear compartments. Bars, 20 μm. (D) Growth of Bac20 EGFPVP22 compared to that of the Bac20 parental virus. Approximately 5×10^5 CESCs were infected with 100 PFU of the respective MDV. At 6, 24, 48, 72, 96, 120, 144, 168, and 192 h postinfection, cells were trypsinized and titers were determined on fresh CESCs (two wells per dilution). Virus plaques were counted at 5 days postinfection under a light microscope. The curves represent the mean value of two independent experiments; error bars indicate the standard deviation of the mean.

the L13a anti-VP22 MAb and an alkaline phosphatase-conjugated secondary antibody. The alkaline phosphatase was detected with a solution made of Nitro Blue tetrazolium chloride and 5-bromo-4-chloro-3-indolyl phosphate (BCIP) (Zymed, South San Francisco, CA). The theoretical molecular mass of EGFPVP22 was estimated with DNA Strider software version 1.4f3.

Immunofluorescence microscopy. MDV EGFPVP22-infected cells analyzed by fluorescence microscopy were prepared by two different procedures. (i) CESCs were grown on glass coverslips coated with gelatin in 24-well plates and infected with EGFPVP22-expressing MDV for 4 or 5 days. (ii) Sorted infected cells (see below for the cell-sorting procedure) were replated on glass coverslips

at a concentration of 10^5 cells/ml for 1.5 h. For both types of plating condition, cells were fixed with 4% paraformaldehyde for 30 min at room temperature, permeabilized with 0.1% Triton X-100, and stained with anti-VP5 MAb F19 (1:1,000), followed by rabbit anti-mouse Alexafluor 594 (1:4,000). The nuclei were stained with Hoechst 33342. Images were captured with Axiovision software (Zeiss, Göttingen, Germany). The imaging system included a charge-coupled device Axiocam MRm camera (Zeiss) and an ApoTome system (Zeiss) mounted on an Axiovert 200M inverted epifluorescence microscope (Zeiss). For cellular localization, the ApoTome system was used with a 63× Plan-Apochromat (NA 1.4) lens (Zeiss).

Virus growth curves. Virus growth curves were determined as described earlier (41). This study was done entirely with primary CESCs. Plaques were counted 5 days postinfection under an Axiovert 25 inverted microscope (Zeiss).

Flow cytometry analysis and cell sorting. MDV EGFPVP22-infected cells were trypsinized, concentrated, and filtered on a 30-μm-pore-size membrane. Cells were then sorted with a MoFlo (DakoCytomation A/S, Fort Collins, CO) high-speed cell sorter equipped with a solid-state laser operating at 488 nm and 100 mW. Debris were eliminated on the basis of morphological criteria. GFP fluorescence was analyzed with a 530/40-nm band-pass filter. The sorting speed was around 20,000 cells/s. For the most accurate sorting, we used the "purified mode" and a droplet envelope of 1 drop. To analyze their viability, we incubated 200,000 of these sorted cells with propidium iodide dye at a final concentration of 10 μg/ml for 10 min and reexamined them by flow cytometry.

TEM. For conventional EM, immediately after running out of the cell sorter, the EGFP-sorted cells were pelleted by low-speed centrifugation and fixed for 16 h in 4% paraformaldehyde and 1% glutaraldehyde in 0.1 M phosphate buffer (pH 7.2). Therefore, for these cells the delay between trypsinization and fixation was about 30 to 60 min. An alternative way of cell preparation was also used. It consisted of replating the EGFP-sorted cells on a 3.5-cm-diameter dish for 3 h, washing them twice in phosphate-buffered saline (PBS), fixing them for 1 h with the fixative described above, and gently scraping them off with a cell scraper. The scraped-off cells were then incubated overnight in the fixative buffer before pelleting. The same EM preparation method was used for both cell pellets and was performed as described earlier (42). Ultrathin sections were cut, placed on EM grids, and stained with 5% uranyl acetate–5% lead citrate. For immuno-EM, EGFP-sorted cells were fixed in a solution containing 4% paraformaldehyde diluted in 0.1 M phosphate buffer (pH 7.2) for 16 h. The pellet was prepared as already described (42). Sections were deposited on gold EM grids coated with collodion membrane. Immunolabeling was then performed on the grids. First, ultrathin sections were blocked with 1% fraction V bovine serum albumin in PBS for 1.5 h. Then, the primary antibody diluted in PBS–1% bovine serum albumin (JL8 anti-EGFP at 1:2,000 or F19 anti-VP5 at 1:1,000) was incubated on the grids for 1.5 h. Diluted 15-nm-diameter gold particles conjugated to goat anti-mouse immunoglobulin G antibodies (EM.GAM15) in PBS–0.1% bovine serum albumin (1:30) were added, and the mixture was incubated for 1 h. The specificity of the reaction was verified with the goat antibody conjugate with no primary antibody and with a primary irrelevant anti-hepatitis C virus MAb (H52). Ultrathin sections were stained as described above. All sections were observed with a JEOL 1010 transmission electron microscope (JEOL, Tokyo, Japan) equipped with a multiscan MSC 792 camera (Gatan, Pleasanton, CA). Images were captured through Digital Micrograph software version 3.11.1 (Gatan).

RESULTS

Construction and analysis of recombinant EGFPVP22-expressing MDV. The UL49 gene expressing the VP22 tegument protein is located in the unique long region of MDV. The entire EGFPUL49 fusion gene, which encodes EGFPVP22, was inserted into plasmid pUL48-50 Stu (Fig. 1A). The resulting shuttle plasmid, pUL48-50 EGFPUL49, was cotransfected into CESCs together with the mutant Bac20ΔUL49 DNA. The Bac20ΔUL49 virus is replication deficient and does not produce viral plaques in CESCs (16). Therefore, the formation of plaques after the cotransfection of BACmid Bac20ΔUL49 with plasmid pUL48-50 EGFPUL49 strongly suggests that all VP22 functions were rescued. The rescuing fluorescent virus, named Bac20 EGFPVP22, was grown for the production of a master stock of cell-associated virus and for further analyses. The correct insertion of the EGFPUL49 gene in the Bac20 genome was verified by PCR and sequencing of the UL49 region from extracted viral DNA (data not shown). To analyze the expression of the EGFPVP22 protein in infected cells, CESCs were infected with Bac20 EGFPVP22 for 5 days and protein expression was analyzed by Western blot assay with an anti-GFP or an anti-VP22 antibody. In both cases, we detected a unique band with an apparent molecular mass of 50 kDa, a value close to the theoretical molecular mass calculated with DNA Strider 1.4 software (Fig. 1B). MDV EGFPVP22-infected cells were then examined by fluorescence microscopy at 5 days postinfection. A representative picture of a plaque is shown in Fig. 1C. EGFPVP22 cell localization was heterogeneous, in both the cytoplasmic and nuclear cell compartments. These fluorescence experiments showed that the subcellular localization of EGFPVP22 in infected cells did not differ from that of untagged VP22 in a viral context (16). Moreover, 97% (97/100) of the EGFPVP22-positive cells were also found to be positive for the VP5 antigen. This result indicated that EGFP-positive cells were at a late stage of infection.

Lastly, to assess the rate of Bac20 EGFPVP22 replication, growth kinetics experiments with the Bac20 EGFPVP22 virus and the parental Bac20 virus were carried out with CESCs. CESCs were infected at 100 PFU and harvested at various times from 1 to 192 h postinfection, and titers were determined on fresh CESCs. Compared to the parental virus, growth of the Bac20 EGFPVP22 virus was slightly impaired at all of the time points measured (Fig. 1D). For each point, we calculated the ratio (mean number of plaques for the wild type/mean number for the mutant), and the median ratio was 3.2. Despite this approximately threefold decrease in viral growth, this mutant still replicated quite efficiently in cell culture and made a suitable tool for our morphogenesis study.

Cell sorting of MDV EGFPVP22-infected cells by flow cytometry. Cells infected with Bac20 EGFPVP22 for 5 days were trypsinized and analyzed by flow cytometry. Overall, 7% to 16% of the cells expressed EGFPVP22, depending on the experiment (Fig. 2A, parts a and b). Only highly fluorescent cells were sorted with a preparative (Mo-Flo) flow cytometer. Analysis by cytometry showed that 98% of the sorted cells were EGFP positive, with an side scatter compatible with poorly damaged cells (Fig. 2A, parts c and d). The high viability of these EGFP-labeled cells (>95%) was confirmed by a propidium iodure labeling method. An aliquot of the sorted cells was plated on glass coverslips and analyzed by fluorescence microscopy. VP5 staining of these cells showed that more than 90% of the cells were positive for EGFPVP22 and the VP5 capsid protein. Moreover, the sorted cells presented localization patterns of EGFPVP22 fluorescence and VP5 staining similar to those of unsorted cells plated at a low density (not shown). Lastly, these cells were also used several times to infect a fresh CESC layer by coculture and they remained infectious (not shown). Overall, these data suggest that the sorting method used was efficient at purifying live, EGFPVP22-positive cells and did not affect the phenotype or infectiosity of the infected cells. Hence, this procedure allowed the purification of MDV-infected cells expressing late viral antigens and was suitable for subsequent analyses by TEM.

TEM of MDV EGFPVP22 sorted cells. No extracellular MDV particles were observed, despite a careful examination of more than 200 MDV-infected cells. All other stages of assem-

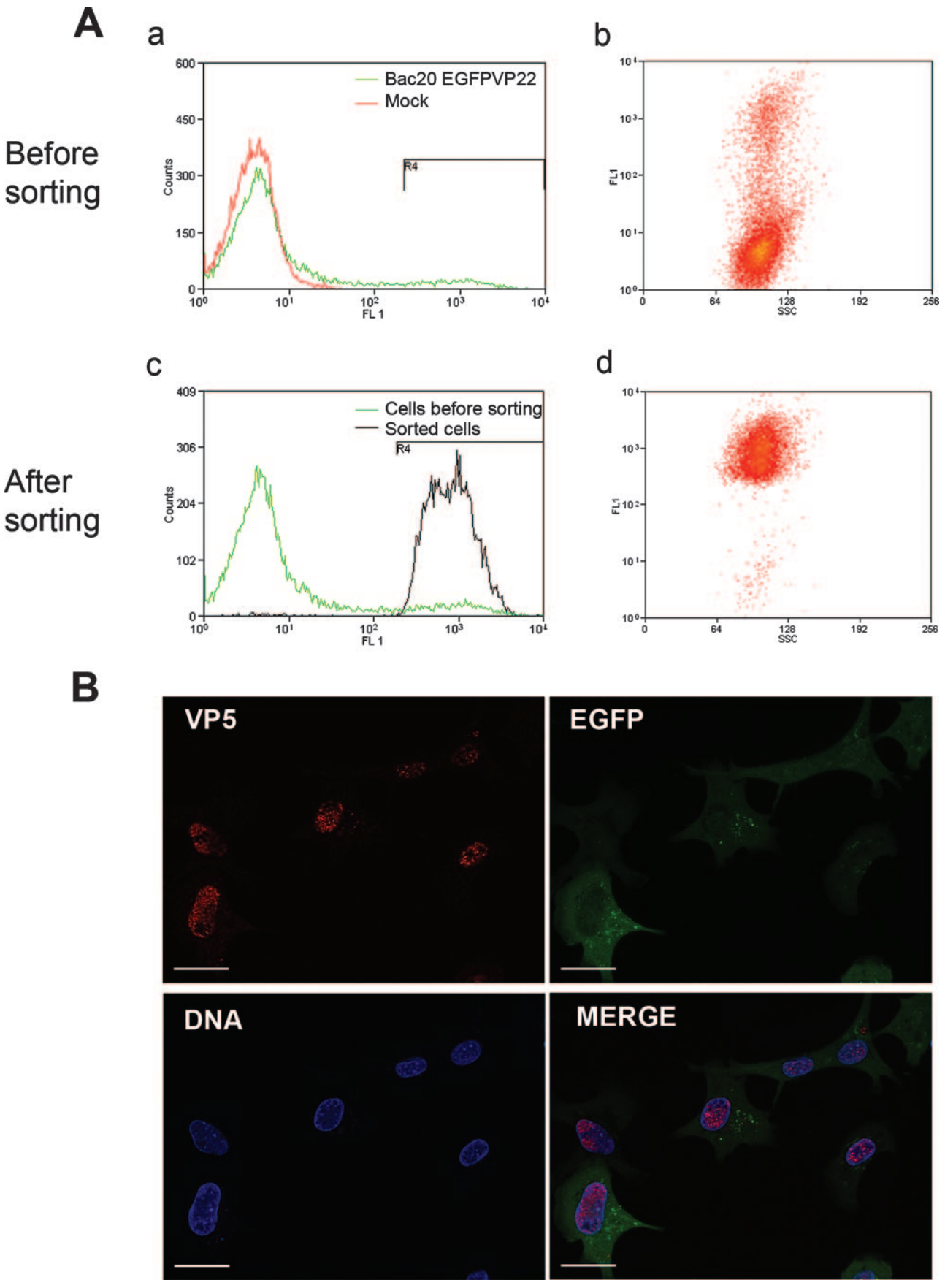
A
a
b
Before sorting
Bac20 EGFPVP22
Mock
R4
Counts
FL 1
FL1
SSC
c
d
After sorting
Cells before sorting
Sorted cells
B
VP5
EGFP
DNA
MERGE

bly and egress could readily be visualized, although never in the same cell section. An overview of two infected cells with examples of intranuclear, perinuclear, and cytoplasmic virus particles is shown in Fig. 3.

The ultrastructure of the intranuclear capsids appeared to be similar to that described for other herpesviruses (24, 44). The A, B, and C capsid types were detected, usually dispersed as isolated capsids in the nucleoplasm (Fig. 4A, part a). The sizes of the type C capsids ranged between 94 and 102 nm in diameter. We also observed many small, round structures around 35 nm in diameter, which are commonly termed small particles. No pseudocrystal of capsids was detected as previously described for HSV-1 or PRV (24, 44). The presence of VP5 in these nuclear capsids was confirmed by immuno-EM with the F19 MAb anti-VP5. A relatively intense gold labeling restricted to the capsids was observed (Fig. 4A, part b).

Primary enveloped virions were rarely observed (Fig. 4B, part a). Their morphology was comparable to that already described for other alphaherpesviruses, with a centrally located nucleocapsid, of either type B or C, surrounded by a smooth and thick electron-dense envelope. Furthermore, primarily enveloped virions exhibited a uniform diameter of between 130 and 160 nm. They were clearly located in the perinuclear space or in vacuoles in the vicinity of the nucleus (Fig. 4B, part a). The latter position most likely represents virions in a perinuclear cleft which originated from either an oblique cut or the irregular shape of the nuclear membrane, which can also form invaginations. No deenvelopment or budding at the outer nuclear membrane was observed. Some single capsidless vesicles of the same size (in diameter) were regularly observed in the perinuclear space (Fig. 4B, parts b to e), even more frequently than vesicles with capsids (data not shown). The only fusion event observed at the outer nuclear membrane level is shown in Fig. 4B, part e, and seemed to concern a capsidless vesicle. Curiously, accumulations of enveloped virions in the perinuclear space were occasionally visualized (Fig. 4B, parts b and c). As already observed with the delU_S3 mutant (46), the inner nuclear membrane became extended into the nucleus, forming invaginations also described as nuclear vacuoles (43). In these accumulations, the envelope of some particles is in continuity with the internal nuclear envelope still attached by a peduncle.

Intracytoplasmic naked capsids were observed either isolated (Fig. 3) or in clusters (Fig. 3 and 5), most frequently in the vicinity of the Golgi apparatus and/or mitochondria. Most of these cytoplasmic capsids were of type C, but type B capsids were sometimes also observed (Fig. 5A). In some instances, these naked capsids were closely associated with or surrounded by electron-dense structures that could be tegument material (Fig. 5B and C). The presence of EGFPVP22 in these electron-dense structures was analyzed by immuno-EM with an anti-EGFP MAb. Indeed, intense gold labeling was observed in

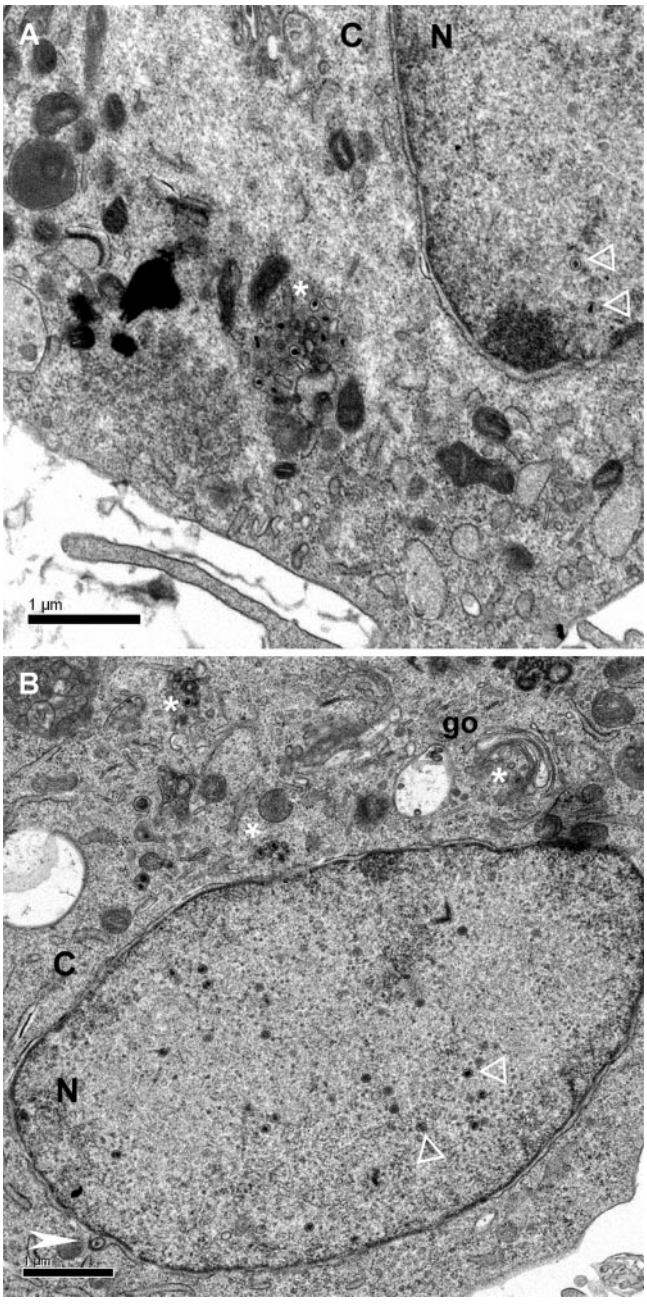

FIG. 3. Overview of CESCs infected with Bac20 EGFPVP22 where most stages of virus assembly and maturation can be observed, except extracellular particles. (A) Nuclear capsids (white open triangles) are visible, as well as an accumulation of cytoplasmic naked capsids (white asterisk) in an electron-dense environment. (B) Multiple nuclear capsids (white open triangles) are visible, as well as an enveloped capsid in the perinuclear cisterna (white arrowhead) and a few naked capsids in the cytoplasm (white asterisk). N, nucleus; C, cytoplasm; go, Golgi complex.

FIG. 2. Analysis of Bac20 EGFPVP22-infected cells before and after cell sorting by cytometry. (A) Flow cytometry analysis scatter plots. CESCs were mock infected or infected with Bac20 EGFPVP22 for 5 days, trypsinized, and analyzed for GFP fluorescence by flow cytometry analysis. In this experiment, 7.5% of the cells were EGFP positive before sorting and 98% were positive after sorting. These results are representative of more than three independent experiments. (B) Fluorescence microscopy analysis of sorted cells. Sorted cells were resuspended in culture medium, plated on glass coverslips for 1.5 h, and fixed with 4% paraformaldehyde. Cells were stained with anti-VP5 MAb F19 (red) and Hoechst 33342 dye (blue). Cells were examined with a Zeiss microscope with the ApoTome system. Overall, 90% of the cells were found to be positive for the EGFPVP22 and VP5 proteins. Bars, 20 μm.

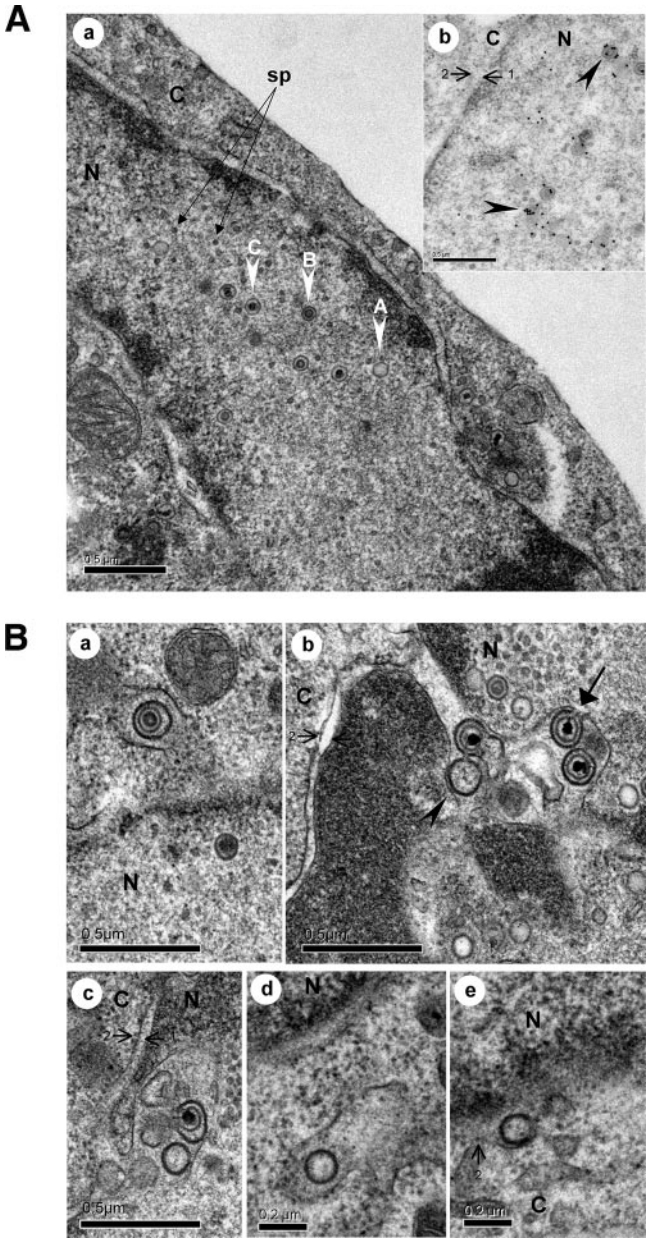

FIG. 4. Nucleocapsids and egress from the nucleus. (A) The three types of capsids (A, B, and C) were detected in the nucleus. In this picture, the C nucleocapsids range from 94 to 102 nm in diameter. Small round particles, termed small particles (sp), frequently reported to be associated with herpesvirus nuclear capsids are indicated by arrows. The inset (part b) shows nuclear capsids exhibiting strong labeling with an anti-VP5 MAb (black arrowheads). (B) Egress from the nucleus. In part a, one single enveloped B nucleocapsid was observed in the perinuclear space as the vacuole membrane seemed to be a continuation of the outer nuclear membrane. This primary enveloped virion had a diameter of approximately 150 nm. Part b shows the accumulation of four enveloped MDV particles in the perinuclear cisterna, including a capsidless particle (black arrowhead) and three particles with an electron-dense core (C capsids). For one of these virions, the primary envelope is in continuity with the inner nuclear envelope (black arrow). The enveloped particles with capsids ranged from 131 to 157 nm in diameter. In part c, an additional image of such perinuclear accumulation of particles is shown. In parts d and e, capsidless particles in a vacuole in proximity to the nucleus and fused to the outer membrane of the nuclear envelope are shown. N, nucleus; C, cytoplasm. The inner membrane (arrow 1) and outer membrane (arrow 2) of the nuclear envelope are indicated.

these structures (Fig. 5C and D), indicating that the electron-dense structures represented accumulations of tegument proteins.

Partially wrapped and fully enveloped cytoplasmic capsids were seldom detected (Fig. 6). No more than one cytoplasmic enveloped virion could be observed in a single cell section. In enveloped virions, the capsid could appear eccentric. The size of the cytoplasmic enveloped particles was estimated to be between 153 by 210 nm (Fig. 6C) and 175 by 274 nm (Fig. 6D). Beneath the envelope, an electron-dense layer was observed on fully enveloped particles. Surface projections indicative of glycoproteins were rarely visible (Fig. 6A).

To quantify these observations, 103 consecutive cell sections were examined by TEM. At least one viral capsid was observed in 90 cells (87.3% of the cells examined). This result is in accordance with the percentage of VP5-positive sorted cells previously quantified by fluorescence. Of these 90 capsid-positive cells, 87 (96.6%) had capsids in their nucleoplasm while not more than 3 (3.3%) had capsids only in their cytoplasm, confirming that most of the cells examined were in a late stage of infection. Next, the numbers of intranuclear, perinuclear, and cytoplasmic nonenveloped and enveloped capsids were recorded. The results of this experiment are summarized in Table 1. Only 4 fully enveloped particles were recorded in the cytoplasm of cell sections that contained 80 unenveloped particles. The percentage of virus particles in each compartment was 90.54% in the nucleus, 0.22% in the perinuclear space, and 9.24% in the cytoplasm. Therefore, the number of virus particles in the nucleus was 10 times higher than that in the cytoplasm.

We could not totally exclude the possibility that the absence of extracellular particles in these samples was due to virus damage or washing out, resulting from cell trypsinization (shortly before sorting) and/or cell sorting. This prompted us to seed the sorted cells on a plate and incubate them for 3 h before fixation for EM preparation in order to let the viruses exit at the cell surface on the basis of the hypothesis that extracellular virions would have been lost in the sorting procedure. Nevertheless, TEM analysis of this sample also revealed an absence of extracellular virus particles (data not shown).

DISCUSSION

While MDV shares many features of replication with the other alphaherpesviruses, it also exhibits some biological peculiarities. In particular, MDV is the only alphaherpesvirus for which no infectivity can be recovered from supernatants and cell lysates. Providing a complete morphogenesis study is therefore crucial to the exploration of this peculiarity. One of the major obstacles to a full understanding of MDV assembly and egress has been the inability to analyze a sufficient number of infected cells at late stages of virus replication. The development of the GFP technology combined with cytometry allows the selection of cells expressing GFP or GFP-tagged proteins. In this report, we present the first ultrastructural study of MDV by the use of a recombinant virus expressing a GFP-tagged tegument viral protein. Infection with this virus allows the production of highly fluorescent infected

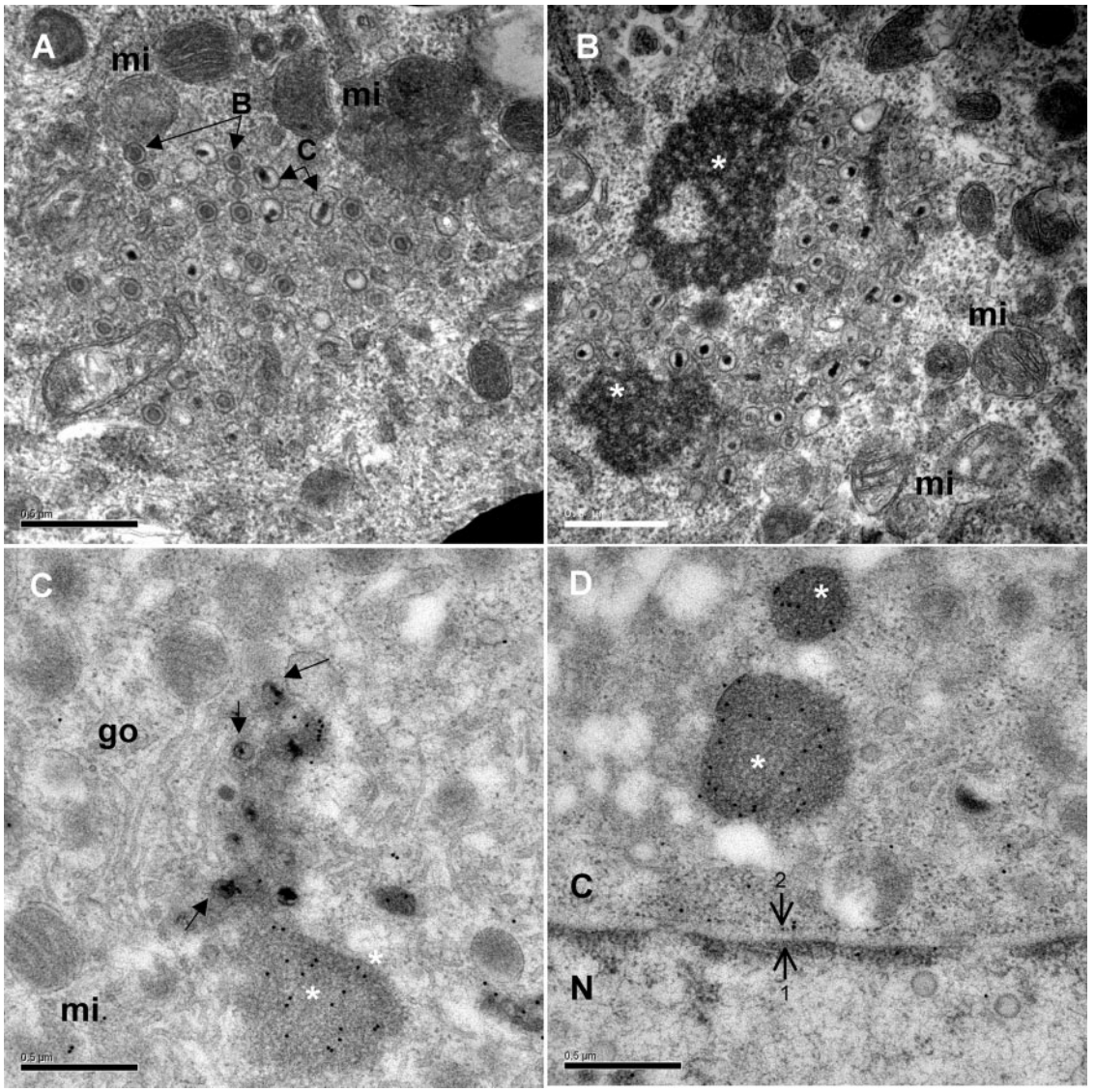

FIG. 5. Accumulation in the cytoplasm of naked capsids and electron-dense material. Naked capsids were present within the cytoplasm either alone or in clusters. Naked capsids were often in the vicinity of mitochondria (mi) or Golgi stacks (go) (panels A, B, and C). Electron-dense material (white asterisk) was also frequently observed in cytoplasmic areas (panels B, C, and D). Although type C capsids were more numerous in the cytoplasm, type B capsids were also readily observed (panel A). Black arrows indicate some naked capsids. (C and D) The cytoplasmic electron-dense material was strongly labeled with the EGFP MAb, whereas other cytoplasmic regions and naked capsids were not. Bars, 0.5 μm. N, nucleus; C, cytoplasm. The inner membrane (arrow 1) and outer membrane (arrow 2) of the nuclear envelope are indicated.

cells at a late stage of infection which can be identified and sorted by cytometry.

The protein to which EGFP was fused for the tracing of infected cells is the major tegument protein VP22. We have previously demonstrated that VP22 is abundantly expressed in infected CESCs (15) and that the gene that encodes this protein is essential for MDV growth in cell culture (16). We show here that the addition of the EGFP coding sequence to the 5′ end of the VP22 open reading frame decreases MDV replication in cell culture approximately threefold. Since UL49 is absolutely essential for MDV replication in cell culture, it is not surprising that a modification of its viral growth is detectable when a tag is fused at one of its ends, in contrast to PRV, HSV-1, or BHV-1, for which UL49 is not essential (13, 19; V. A. Lobanov, C. Zheng, L. A. Babiuk, and S. van Drunen Littel-van den Hurk, 32nd International Herpesvirus Workshop, 2007). The fact that this recombinant virus is still highly replicative suggests that a free N terminus is not absolutely essential for VP22 function but could be involved in its efficiency. There are various possible reasons for this reduction in functional efficiency, such as an alteration of the overall VP22 tridimensional structure, an incomplete posttranslational modification, or reduced accessibility to potential interaction partners. This last hypothesis is compatible with a role for HSV-1 VP22 in the incorporation of several viral proteins into mature virions that may act subsequently at the early stages of infec-

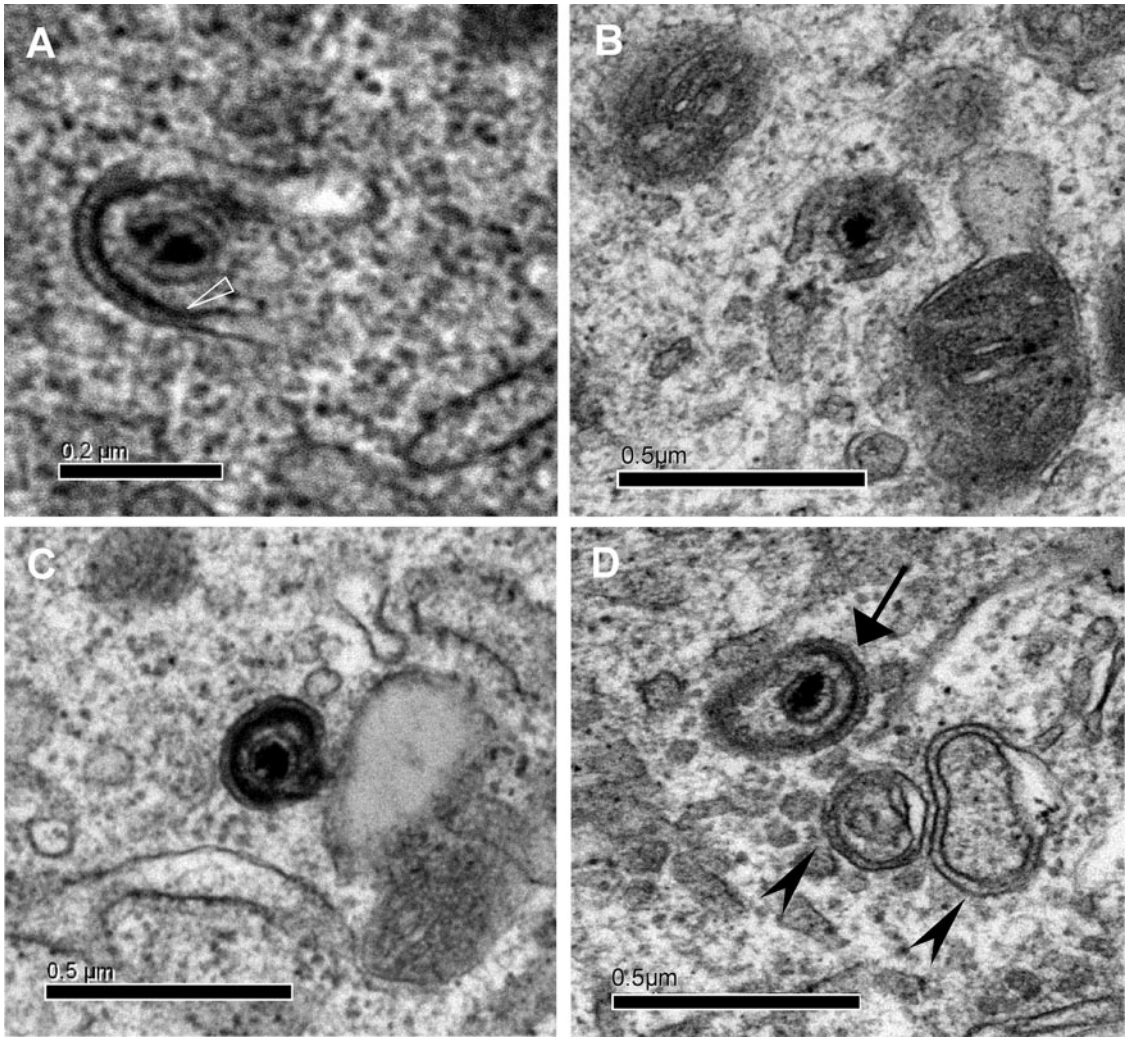

FIG. 6. Partially wrapped and fully enveloped cytoplasmic capsids. (A and B) MDV capsids in the process of being wrapped. In panel A, a thickening under the inside membrane (white open triangle) highly dense to electrons may represent the tegument. Between the two membranes, spikes are visible. (C) A distinct fully enveloped particle with a size of 210 by 153 nm. (D) An enveloped capsid (arrow) detectable together with two empty large vesicles (arrowheads).

tion (17, 18). For MDV, the presence of EGFP at the N terminus of VP22 may also affect virion composition and therefore recombinant virus replication.

The morphogenesis study described here was exclusively performed with a VP22 recombinant MDV after trypsinization and cell separation. While we cannot exclude the possibility that these parameters could influence our findings on virion morphogenesis, several arguments lead us to think that these factors did not influence our morphogenesis results. (i) With respect to the impact of cell sorting, our fluorescence microscopy analyses indicate that cell separation does not affect the location of several viral markers when the cells are reseeded. Moreover, the infectivity associated with these cells is preserved (not shown), showing that these cells can still produce infectious virions. One can also suspect that the trypsinization step has damaged viruses associated with the plasma membrane outside and that cell sorting has washed out the free particles. These effects are unlikely for two major reasons. The 3-h replating step was theoretically sufficiently long to let intracellular enveloped virions exit into the outer environment, if this phenomenon should happened. For various protein reporters, the exocytosis process takes less than 1 h between the trans-Golgi network and the cell surface (29, 33). Also, other enveloped viruses like retroviruses can be observed in the extracellular space after comparable cell-sorting procedures,

TABLE 1. Numbers and percentages of nuclear, perinuclear, and cytoplasmic capsids in capsid-positive cells[a]

Total no. of particles counted	No. (%) of nuclear B and C capsids	No. (%) of perinuclear virions with DNA[b]	No. (%) of cytoplasmic virions	
			Naked	Enveloped
909	823 (90.54)	2 (0.22)	80 (8.80)	4 (0.44)

[a] Ninety cells with at least one capsid were examined for this quantification.
[b] Does not include virus particles in perinuclear accumulations.

suggesting that this technique does not impair the detection of extracellular virions (C. Denesvre, personal observations). The only consequence of the cell sorting observed was the absence of large multinucleated cells due to the cell filtration through 30-μm-pore-size membranes to avoid clogging of the cell sorter pipes. Therefore, we believe that this cell separation process does not have a major influence on MDV morphogenesis and therefore did not affect our results, including the absence of extracellular virions. (ii) The impact of the VP22 mutation is more difficult to evaluate because of the essential role of this protein in MDV replication and spreading. However, in HSV-1 and PRV, a fusion protein consisting of GFP and the homologous VP22 protein (GFP-VP22) is incorporated into virions with the same efficiency as VP22 (13, 19). Moreover, to date, a lack of VP22 is not associated with a defect in virion morphogenesis for other alphaherpesviruses. For example, an UL49-null HSV-1 mutant did not exhibit decreased production of intracellular virions (17). Therefore, we suspect that the decrease in replication observed for the EGFPVP22-expressing MDV mutant is due to an impairment in the early steps rather than in those of morphogenesis.

On the basis of their morphology and location, we observed all types of intracellular particles described for the other herpesviruses, i.e., naked nuclear and cytoplasmic capsids, as well as the primarily and secondarily enveloped virions. Their characteristics are in accordance with those described for other alphaherpesviruses (22, 25) or even for wild-type MDV (1). One exception, however, concerns the cytoplasmic enveloped particles, for which we calculated a size of between 152 and 273 nm. Although this size is in the same range as that described for HSV-1, PRV, equid herpesvirus 1, and VZV (22, 25), it is significantly smaller than that previously shown for MDV (5). Indeed, in this first report, MDV virions extracted from lysed feather follicle epitheliums had a diameter of 273 to 400 nm. This difference may be due to differences in preparation techniques, as Calnek and colleagues harvested virions from tissues by using distilled water and freeze-thaw cycles. This process may have artificially increased the size of the virions by an osmotic phenomenon.

Although they were present, primary enveloped virions were only rarely observed, as with other alphaherpesviruses grown in cell culture (22, 25). These primary enveloped virions support the model of egress of nucleocapsids from the nucleus by budding at the inner nuclear membrane. In the present study, we made the striking observation of few accumulations of enveloped virions in the perinuclear space with an invagination of the inner nuclear membrane into the nucleus. This phenomenon is usually associated with deletion of the U_S3 gene. A recent study with Bac20 wild-type MDV in chicken embryo cells reported no accumulation of such primary enveloped virions in the perinuclear space (46). The difference between these two studies might be due to the number of cells examined (three times higher in the present study) or to the cell culture system used (skin cells versus fibroblasts). The CESCs used in the present study contain mostly fibroblasts but also myoblasts and keratinocytes (not shown). Curiously, one intranuclear vacuole containing two primary enveloped particles was also observed in the skin of a chicken experimentally infected with MDV (9). This type of observation was also noted for VZV in melanocytes (25). We therefore hypothesize that such features might be associated with a particular cell type derived from the skin. Because this phenotype is usually associated with the U_S3 gene and since U_S3 is present in the Bac20 EGFPVP22 genome, it is conceivable that U_S3 is either not expressed or not functional in some types of cells or that exit from the nucleus is decelerated in these cells. Unfortunately, the association between a defect in kinase activity and some cell types appears to be difficult to explore in such a small subset of cells.

In this study, 823 nucleocapsids were observed in the nucleus whereas only 80 naked capsids and 4 enveloped capsids were counted in the cytoplasm. A previous quantification of nuclear and cytoplasmic capsids was performed by Schumacher and colleagues with wild-type Bac20 in CEC layers infected for 3 days (46). They found 75% intranuclear capsids for 24% cytoplasmic ones in 38 cells examined with a total of 248 particles. This cytoplasmic particle percentage is 2.5-fold higher than that found in our study. Nevertheless, a strict comparison of those two percentages is difficult because many parameters are different, like the viruses, primary cells, and infection times used. Moreover, in the report of Schumacher et al. it is not clear whether they counted the cytoplasmic capsids only in cells also presenting nuclear capsids and if they did not compatibilize infected cells at early stages of infection. In that case, they would have overestimated the number of cytoplasmic capsids. However, in our two studies, the number of total cytoplasmic particles compared to that in the nucleus suggests that exit from the nucleus was not very efficient. The hypothesis of rapid movement of the particles from the nucleus to the cell surface can be eliminated because of the absence of detectable extracellular particles. In the cytoplasm, the relatively high number of naked particles compared to that of enveloped particles without extracellular virions indicates that the late stage of egress is also very inefficiently achieved. However, our data do not allow us to conclude whether this is due to a deficiency in the secondary envelopment and/or in virus transport and maturation through the exocytosis pathway. Moreover, the very low number of enveloped MDV virions in the cytoplasm shows that, in this respect, MDV is different from VZV, for which such particles are numerous (25). This observation is crucial and can explain why for MDV, unlike for VZV and even the closely related turkey herpesvirus, infectious virions cannot be recovered from cell lysates by freeze-thawing or sonication. These results are in good agreement with the current dogma that living cells are absolutely necessary for MDV infection and for vaccine preparation. Any way leading to an accumulation of intracytoplasmic enveloped MDV virions may allow the purification of infectious virions and improve vaccine production processes. Finally, although we could not detect extracellular particles despite extensive EM observations, we cannot totally exclude the possibility of their presence. However, if this phenomenon exists, its frequency is certainly very low. In this study, we clearly observed pictures of capsid wrapping in cytoplasmic membranes with an electron-dense material underneath. Our images of this stage support the acquisition of tegument and envelope to form mature virions in the cytoplasm rather than through the luminal pathway. It is unlikely that these capsids were particles just going out from a vesicle during the entry process for two reasons. First, we observed cells at late stages of infection probably refractory to new infections because of the interference phenomenon. Sec-

ond, the tegument-like dense material associated with the invaginated vesicle membrane is usually not visible during the entry process. Regarding exit from the nucleus, we clearly observed the budding of particles from the inner nuclear membrane, some particles in the perinuclear area, and a single fusion event with the outer membrane of the nuclear envelope for a capsidless particle. These observations suggest that MDV can exit from the nucleus through the envelopment-deenvelopment process at the level of the nuclear membranes, rather than through nuclear pore enlargement events never observed in this study. Further biochemical studies need to be performed to prove that MDV indeed uses the double-envelopment pathway for its morphogenesis.

The absence of extracellular virions raises the question of the cell-to cell spreading mechanism of MDV. One hypothesis predicts that cell-to-cell spreading does not occur through release of mature virions but only through cellular junctions, a phenomenon that could not be observed in this study because of the cell-sorting strategy used and the absence of noninfected cells. Such a pathway of cell-to-cell spreading has been demonstrated between T lymphocytes for the human T-cell leukemia virus HTLV-1, a retrovirus which also requires living cells for spreading (26). Such a pathway is currently under examination with the MDV mutant described here.

ACKNOWLEDGMENTS

We thank A. Francineau for technical assistance with all of our cell culture experiments. We thank C. Fortin for constructing plasmid p48-50 Stu. We also thank B. Arbeille and D. Kerboeuf for advice on EM and cytometry. We thank S. Trapp and L. Fragnet for comments on the manuscript.

Our data were generated with the help of the RIO EM facility of François Rabelais University. C. Blondeau was supported by an INRA/Region Centre fellowship. This work was supported by a grant from the Region Centre (France). The three laboratories that participated in this study are members of a federative research institute on infectious diseases, IFR136.

REFERENCES

1. **Biggs, P. M.** 2001. The history and biology of Marek's disease virus. Curr. Top. Microbiol. Immunol. **255:**1–24.
2. **Biggs, P. M., and L. N. Payne.** 1967. Studies on Marek's disease. 1. Experimental transmission. J. Natl. Cancer Inst. **39:**267–280.
3. **Blondeau, C., N. Chbab, C. Beaumont, K. Courvoisier, N. Osterrieder, J.-F. Vautherot, and C. Denesvre.** 2007. A full UL13 open reading frame in Marek's disease virus (MDV) is dispensable for tumor formation and feather follicle tropism and cannot restore horizontal virus transmission of rRB-1B in vivo. Vet. Res. (Paris) **38:**419–433.
4. **Bublot, M., and J. M. Sharma.** 2004. Vaccination against Marek's disease, p. 168–185. *In* F. Davison and V. K. Nair (ed.), Marek's disease. An evolving problem. Elsevier Academic Press, Compton, United Kingdom.
5. **Calnek, B. W., H. K. Adldinger, and D. E. Kahn.** 1970. Feather follicle epithelium: a source of enveloped and infectious cell-free herpesvirus from Marek's disease. Avian Dis. **14:**219–233.
6. **Campadelli-Fiume, G., F. Farabegoli, S. Di Gaeta, and B. Roizman.** 1991. Origin of unenveloped capsids in the cytoplasm of cells infected with herpes simplex virus 1. J. Virol. **65:**1589–1595.
7. **Campadelli-Fiume, G., and T. Gianni.** 2006. HSV glycoproteins and their roles in virus entry and egress, p. 135–156. *In* R. M. Sandri-Goldin (ed.), Alpha herpesviruses. Caister Academic Press, Norfolk, United Kingdom.
8. **Campadelli-Fiume, G., and B. Roizman.** 2006. The egress of herpesviruses from cells: the unanswered questions. J. Virol. **80:**6716–6717. (Letter.)
9. **Cho, K.-O., K. Ohashi, and M. Onuma.** 1999. Electron microscopic and immunohistochemical localization of Marek's disease (MD) herpesvirus particles in MD skin lymphomas. Vet. Pathol. **36:**314–320.
10. **Churchill, A. E., and P. M. Biggs.** 1967. Agent of Marek's disease in tissue culture. Nature **215:**528–530.
11. **Cilloniz, C., W. Jackson, C. Grose, D. Czechowski, J. Hay, and W. T. Ruyechan.** 2007. The varicella-zoster virus (VZV) ORF9 protein interacts with the IE62 major VZV transactivator. J. Virol. **81:**761–774.
12. **Coudert, F., and L. Cauchy.** 1975. Virus replication and cell modifications in organ cultures of tumor tissue from chickens with Marek's disease. J. Natl. Cancer Inst. **55:**47–51.
13. **del Rio, T., T. H. Ch'ng, E. A. Flood, S. P. Gross, and L. W. Enquist.** 2005. Heterogeneity of a fluorescent tegument component in single pseudorabies virus virions and enveloped axonal assemblies. J. Virol. **79:**3903–3919.
14. **del Rio, T., H. C. Werner, and L. W. Enquist.** 2002. The pseudorabies virus VP22 homologue (UL49) is dispensable for virus growth in vitro and has no effect on virulence and neuronal spread in rodents. J. Virol. **76:**774–782.
15. **Dorange, F., S. El Mehdaoui, C. Pichon, P. Coursaget, and J. F. Vautherot.** 2000. Marek's disease virus (MDV) homologues of herpes simplex virus type 1 UL49 (VP22) and UL48 (VP16) genes: high-level expression and characterization of MDV-1 VP22 and VP16. J. Gen. Virol. **81:**2219–2230.
16. **Dorange, F., B. K. Tischer, J. F. Vautherot, and N. Osterrieder.** 2002. Characterization of Marek's disease virus serotype 1 (MDV-1) deletion mutants that lack UL46 to UL49 genes: MDV-1 UL49, encoding VP22, is indispensable for virus growth. J. Virol. **76:**1959–1970.
17. **Duffy, C., J. H. LaVail, A. N. Tauscher, E. G. Wills, J. A. Blaho, and J. D. Baines.** 2006. Characterization of a UL49-null mutant: VP22 of herpes simplex virus type 1 facilitates viral spread in cultured cells and the mouse cornea. J. Virol. **80:**8664–8675.
18. **Elliott, G., W. Hafezi, A. Whiteley, and E. Bernard.** 2005. Deletion of the herpes simplex virus VP22-encoding gene (UL49) alters the expression, localization, and virion incorporation of ICP0. J. Virol. **79:**9735–9745.
19. **Elliott, G., and P. O'Hare.** 1999. Live-cell analysis of a green fluorescent protein-tagged herpes simplex virus infection. J. Virol. **73:**4110–4119.
20. **Enquist, L. W., P. J. Husak, B. W. Banfield, and G. A. Smith.** 1998. Infection and spread of alphaherpesviruses in the nervous system. Adv. Virus Res. **51:**237–347.
21. **Fuchs, W., H. Granzow, and T. C. Mettenleiter.** 2003. A pseudorabies virus recombinant simultaneously lacking the major tegument proteins encoded by the UL46, UL47, UL48, and UL49 genes is viable in cultured cells. J. Virol. **77:**12891–12900.
22. **Granzow, H., B. G. Klupp, W. Fuchs, J. Veits, N. Osterrieder, and T. C. Mettenleiter.** 2001. Egress of alphaherpesviruses: comparative ultrastructural study. J. Virol. **75:**3675–3684.
23. **Granzow, H., B. G. Klupp, and T. C. Mettenleiter.** 2004. The pseudorabies virus US3 protein is a component of primary and of mature virions. J. Virol. **78:**1314–1323.
24. **Granzow, H., F. Weiland, A. Jöns, B. G. Klupp, A. Karger, and T. C. Mettenleiter.** 1997. Ultrastructural analysis of the replication cycle of pseudorabies virus in cell culture: a reassessment. J. Virol. **71:**2072–2082.
25. **Harson, R., and C. Grose.** 1995. Egress of varicella-zoster virus from the melanoma cell: a tropism for the melanocyte. J. Virol. **69:**4994–5010.
26. **Igakura, T., J. C. Stinchcombe, P. K. Goon, G. P. Taylor, J. N. Weber, G. M. Griffiths, Y. Tanaka, M. Osame, and C. R. Bangham.** 2003. Spread of HTLV-I between lymphocytes by virus-induced polarization of the cytoskeleton. Science **299:**1713–1716.
27. **Johnson, D. C., and M. T. Huber.** 2002. Directed egress of animal viruses promotes cell-to-cell spread. J. Virol. **76:**1–8.
28. **Johnson, E. A., C. N. Burke, T. N. Fredrickson, and R. A. DiCapua.** 1975. Morphogenesis of Marek's disease virus in feather follicle epithelium. J. Natl. Cancer Inst. **55:**89–99.
29. **Kaether, C., and H. H. Gerdes.** 1995. Visualization of protein transport along the secretory pathway using green fluorescent protein. FEBS Lett. **369:**267–271.
30. **Kingston, E.** 2001. Introduction of DNA into mammalian cells, p. 9.0.1–9.1.11. *In* F. M. Ausubel, R. Brent, R. E. Kingston, D. D. Moore, J. G. Seidman, J. A. Smith, and K. Struhl (ed.), Current protocols in molecular biology, vol. 1. John Wiley & Sons, Inc., Boston, MA.
31. **Leuzinger, H., U. Ziegler, E. M. Schraner, C. Fraefel, D. L. Glauser, I. Heid, M. Ackermann, M. Mueller, and P. Wild.** 2005. Herpes simplex virus 1 envelopment follows two diverse pathways. J. Virol. **79:**13047–13059.
32. **Liang, X., B. Chow, Y. Li, C. Raggo, D. Yoo, S. Attah-Poku, and L. A. Babiuk.** 1995. Characterization of bovine herpesvirus 1 UL49 homolog gene and product: bovine herpesvirus 1 UL49 homolog is dispensable for virus growth. J. Virol. **69:**3863–3867.
33. **Matlin, K. S., and K. Simons.** 1983. Reduced temperature prevents transfer of a membrane glycoprotein to the cell surface but does not prevent terminal glycosylation. Cell **34:**233–243.
34. **Mettenleiter, T. C.** 2004. Budding events in herpesvirus morphogenesis. Virus Res. **106:**167–180.
35. **Mettenleiter, T. C.** 2002. Herpesvirus assembly and egress. J. Virol. **76:**1537–1547.
36. **Mettenleiter, T. C., and T. Minson.** 2006. Egress of alphaherpesviruses. J. Virol. **80:**1610–1611. (Letter.)
37. **Mettenleiter, T. C., and T. Minson.** 2006. The egress of herpesviruses from cells: the unanswered questions. J. Virol. **80:**6718–6719. (Authors' reply to letter.)
38. **Nazerian, K., and B. R. Burmester.** 1968. Electron microscopy of a herpes virus associated with the agent of Marek's disease in cell culture. Cancer Res. **28:**2454–2462.

39. **Nazerian, K., J. J. Solomon, R. L. Witter, and B. R. Burmester.** 1968. Studies on the etiology of Marek's disease. II. Finding of a herpesvirus in cell culture. Proc. Soc. Exp. Biol. Med. **127:**177–182.
40. **Nazerian, K., and R. L. Witter.** 1975. Properties of a chicken lymphoblastoid cell line from Marek's disease tumor. J. Natl. Cancer Inst. **54:**453–458.
41. **Parcells, M. S., A. S. Anderson, J. L. Cantello, and R. W. Morgan.** 1994. Characterization of Marek's disease virus insertion and deletion mutants that lack US1 (ICP22 homolog), US10, and/or US2 and neighboring short-component open reading frames. J. Virol. **68:**8239–8253.
42. **Patient, R., C. Hourioux, P. Y. Sizaret, S. Trassard, C. Sureau, and P. Roingeard.** 2007. Hepatitis B virus subviral envelope particle morphogenesis and intracellular trafficking. J. Virol. **81:**3842–3851.
43. **Poon, A. P., L. Benetti, and B. Roizman.** 2006. U_S3 and $U_S3.5$ protein kinases of herpes simplex virus 1 differ with respect to their functions in blocking apoptosis and in virion maturation and egress. J. Virol. **80:**3752–3764.
44. **Roizman, B., and A. E. Sears.** 1996. Herpes simplex viruses and their replication, p. 1043–1107. *In* B. N. Fields, D. M. Knipe, and P. M. Howley (ed.), Fundamental virology, third ed. Lippincott-Raven Publishers, Philadelphia, PA.
45. **Schumacher, D., B. K. Tischer, W. Fuchs, and N. Osterrieder.** 2000. Reconstitution of Marek's disease virus serotype 1 (MDV-1) from DNA cloned as a bacterial artificial chromosome and characterization of a glycoprotein B-negative MDV-1 mutant. J. Virol. **74:**11088–11098.
46. **Schumacher, D., B. K. Tischer, S. Trapp, and N. Osterrieder.** 2005. The protein encoded by the U_S3 orthologue of Marek's disease virus is required for efficient de-envelopment of perinuclear virions and involved in actin stress fiber breakdown. J. Virol. **79:**3987–3997.
47. **Sinzger, C., J. Knapp, K. Schmidt, M. Kahl, and G. Jahn.** 1999. A simple and rapid method for preparation of viral DNA from cell associated cytomegalovirus. J. Virol. Methods **81:**115–122.
48. **Wild, P.** 2006. Egress of alphaherpesviruses. J. Virol. **80:**1611–1612. (Author's reply to letter.)
49. **Wild, P.** 2006. The egress of herpesviruses from cells: the unanswered questions. J. Virol. **80:**6717–6718. (Author's reply to letter.)
50. **Wild, P., M. Engels, C. Senn, K. Tobler, U. Ziegler, E. M. Schraner, E. Loepfe, M. Ackermann, M. Mueller, and P. Walther.** 2005. Impairment of nuclear pores in bovine herpesvirus 1-infected MDBK cells. J. Virol. **79:** 1071–1083.